Ovarian transcriptome profile from pre-laying period to broody period of Xupu goose

Haorong Qin,[*,1,2] Xiaoming Li,[*,†,1] Jian Wang,[*,†] Guobo Sun,[*,†] Xiaohui Mu,[*,†] and Rongchao Ji[†]

[*]*Jiangsu Agri-animal Husbandry Vocational College, Taizhou, Jiangsu 225300, China; and* [†]*National Waterfowl Gene Bank, Taizhou, Jiangsu 225300, China*

ABSTRACT Xupu goose, a breed from Hunan province, produces high quality and quantity of meat and liver. However, its egg production rate is low, with poor reproductive traits but strong broody performance. These characteristics decrease the economic value of Xupu goose significantly. Here, RNA-seq was used to analyze the transcriptome changes of ovaries of Xupu goose at different stages to explore the molecular mechanism of reproduction from the pre-laying period to the broody period. A total of 258 genes were differentially expressed in the 3 stages. These genes are associated with inflammation, reproduction, mutual recognition and adhesion between cells, and cytoskeleton formation, and so on. In particular, we report, for the first time, the expression patterns of *MRP126, serglycin, TXNIP,* and *FZD2* during the pre-laying, egg-laying, and broody periods of goose ovaries. Functional analysis by GO annotation revealed that GO terms were mainly involved in actin, cell signal transduction and regulation, and cellular components. Three pathways, including focal adhesion (gga04510), ECM-receptor interaction (gga04512), and N-Glycan biosynthesis (gga00510), were significantly enriched in the three groups. These findings provide a basis for further exploration of profiles of goose ovaries to improve egg production of Xupu goose.

Key words: Xupu goose, ovarian transcriptome, pre-laying period, laying period, broody period

INTRODUCTION

Goose grows rapidly with low input requirements to yield highly valuable products. China is an important goose production exporter in the world's goose consumer market to meet the high annual demand for goose meat. However, most goose species have long broody periods which are associated with low egg production. As a result, the economic value of the geese industry declines. China has a number of domesticated geese species, with various unique characteristics. Xupu goose, an excellent breed in Hunan province, has excellent performance on fattening and liver production, therefore, is of high economic value (Dai et al., 2016). However, the annual egg production by Xupu goose is only 30 eggs as compared with Huoyan goose (120 eggs/year) and Sichuan goose (70 eggs/year) (Yao et al., 2019). The high broodiness of the Xupu goose significantly decreases the economic benefits of its breeding.

Broodiness, a unique characteristic of most domestic geese, is associated with atrophy of ovaries and fallopian tubes, which consequently terminate egg production (Romanov et al., 2002). Mounting evidence has shown that various environmental factors, such as length of photoperiod (Marsden et al., 1966; Geng et al., 2014) and environmental temperature (Thomason et al., 1976) induce the nesting behavior of female poultry. Estrogen (E_2), progesterone (P_4), prolactin (**PRL**), vasoactive intestinal peptide (**VIP**), dopamine (**AD**), and follicle-stimulating hormone (**FSH**) secreted by the hypothalamic-pituitary-gonadal axis (Sharp et al., 1984; Onagbesan et al., 2009; Zhou et al., 2010; Yu et al., 2016b) have direct effects on nesting behavior. Heredity is also a fundamental factor that modulates broodiness. Emerging reports demonstrate that broodiness is a polygenic trait regulated by at least 2 dominant autosomal genes, implicated in multiple signal transduction pathways, including GnRH and Wnt pathways (Yu et al., 2016a; Gumułka et al., 2020). Heritability of nesting sex for waterfowl is only 0.116. Conventional genetic breeding methods have some shortcomings, for example, the lower efficiency of genetic breeding in the later period and an increasing in the brooding ability of offspring.

Therefore, it would be imperative to explore the molecular mechanisms underlying reproductive biology of geese. The molecular mechanisms of reproductive biology can be adopted to improve the non-broody goose breeds; this approach would improve the economic value of goose breeding.

RNA-seq is a highly sensitive, high throughput, and genome-wide analysis method compared to conventional DNA microarray analysis. The whole-goose genome map was published in 2015, and it provided a genetic basis for RNA-seq analysis studies on geese breeding. Previous reports indicate that multiple organs such as the pituitary (Ye et al., 2019), uterus, and ovary (Yu et al., 2016b; Liu et al., 2018) regulate the broody behavior. Changes in the ovarian transcriptome during the goose reproductive cycle can be explored with RNA-seq analysis. Although differentially expressed genes, including ND1, heat shock protein 70 (**HSP70**) and MAPK have been reported in previous studies (Gao et al., 2015), the studies only compared the transcriptional changes of the ovaries at 2 stages of the reproductive cycle, such as egg-laying vs. nesting (Xu et al., 2013), egg-laying vs. pre-egg laying (Kang et al., 2009; Ding et al., 2015), and egg-laying vs. confinement (laying period and ceased period) (Luan et al., 2014).

In the present study, we used next-generation sequencing technology to sequence the transcriptome of ovaries and compare changes in pre-laying, laying, and broody stages. RNA-seq approach was employed to explore the dynamic changes of broody-related genes and pathways in the 3 stages of the reproductive cycle. Candidate regulatory genes on the broody behavior were screened out, and related pathways were evaluated through KEGG enrichment and GO enrichment analyses. The findings provide a basis for breeding low nesting geese.

MATERIALS AND METHODS

Ethics Statement

All animal experimental protocols in this study complied with guidelines for animal welfare and were approved by Jiangsu Administrative Committee for Laboratory Animals (Permission number: SYXK-SU-2007-0005).

Animals, Feeding, and Ovarian Collection

Xupu geese were purchased from the National Gene Bank of Waterfowl Resources (Jiangsu, China). Geese were raised on the ground under the same environmental condition. The goose family breeding dwellings are including outdoor water and land sports field and indoor house. The indoor house is equipped with an automatic all-flock feed and water line device. The geese were fed twice daily by an automatic all-flock feed line (8:00, 16:00) with water and all-flock feed based on their age. The indoor temperature, humidity, and lighting time can be adjusted automatically. The geese were subjected to a standard light regimen of 17 h light (17 L:7D) throughout the experimental period. All geese were fasted and deprived of water 12 h before anesthetization with CO_2 following guidelines by Jiangsu laboratory animal welfare. The ovarian samples were obtained from 3 stages of the reproductive cycle (5 geese per group), including the pre-laying period (90 days old, named T1), the egg-laying period (180 days old, named T2), and the broody period (300 days old, named T3) in the afternoon. The whole ovary including the small and large yellow follicles was swiftly sampled and immediately frozen in liquid nitrogen for further analyses.

Total RNA Isolation, cDNA Library Construction, and RNA-seq

Total RNA of follicles was extracted with Triozl reagent (15596-026, Invitrogen, CA) following the manufacturer's protocol. RNA purity and concentration were determined using NanoPhotometer spectrophotometer (NP80, IMPLEN, CA), and Qubit RNA Assay Kit (Q10211, Invitrogen) in Qubit2.0 fluorometer (Q32866, Life Technologies, CA). RNA Nano 6000 Assay Kit (5067-1511, Agilent Technologies, CA) of the Bioanalyzer 2100 system (G2939BA, Agilent Technologies) and 1% agarose gel were used to assess RNA integrity and whether it was degraded.

Total RNA (3 μg) from each sample was purified using poly-T oligo-attached magnetic beads. Pure RNA was fragmented using divalent cations under elevated temperature in NEBNext First Strand Synthesis Reaction Buffer (5X) (E7525S, NEB, MA). AMPure XP system (A63881, Beckman Coulter, Indianapolis, Indiana) was employed to determine cDNA fragment size, and approximately 250 to 300 bp was selected for library construction. Agilent Bioanalyzer 2100 system was used to assess the quality of libraries. Index-coded samples were clustered on a cBot Cluster Generation System (SY-312-2001, Illumina, CA) using TruSeq PE Cluster Kit v3-cBot-HS (PE-401-3001, Illumina). Following cluster generation, library preparations were sequenced on an Illumina Hiseq platform (HiSeq 2500, Illumina) and 125 bp/150 bp paired-end reads were generated.

RNA-Seq Reads Quality Control and Mapping

Raw data in fastq format were processed using in-house Perl scripts to generate clean data for downstream analyses. The content of Q20, Q30, and GC in the clean data was established. We applied Hisat2v2.0.5 to construct the reference genome index and align the clean data to the reference genome. The number of reads mapped to each gene was calculated with the feature-Counts v1.5.0-p3 program.

Screening of Differentially Expressed Genes and Enrichment Analysis

Differential expression analysis of the genes in the three groups (5 biological replicates per group) was performed with the DESeq2 R package (1.16.1). The resulting P-values were adjusted using Benjamini and Hochberg's approach to control the false discovery rate. Differential expression of genes was evaluated using the following thresholds: |log$_2$-fold change| of $\geq$ 1 and an adjusted P-value of $\leq$ 0.05. Gene ontology (**GO**) and Kyoto Encyclopedia of Genes and Genomes (**KEGG**) analyses were performed to determine the key pathways of the differentially expressed genes (**DEGs**). ClusterProfiler R package was used to test the statistical enrichment of DEGs in KEGG pathways and GO terms. P-values less than 0.05 denoted statistical significance.

Quantitative Real-Time PCR

Seven DEGs were selected randomly to validate the result of high-throughput RNA-seq analysis by quantitative real-time PCR (**qRT-PCR**) as previously described (Everaert et al., 2017). qRT-PCR analysis was conducted on the ABI 7500 Real-Time PCR System (4351105, Applied Biosystems, Foster City, Cafeteria) with ChamQ SYBR qPCR Master Mix (2 ×) (Q331-02, Vazyme, Nanjing, China). Thermocycling parameters used for qRT-PCR were as follows: 95°C for 10 min, 40 cycles at 95°C for 10 s, 60°C for 40 s, and 95°C for 15 s, followed by a melting curve from 60°C for 60 s, 95°C for 30 s, and 60°C for 15 s. Gene expression values were estimated using the $2^{-\Delta\Delta Ct}$ method and normalized using *GADPH*.

RESULTS

Transcriptome Analysis of Ovary From the Geese During the Pre-laying period, Egg-laying Period, or Broody Period

RNA-seq method was employed to explore the transcriptional difference of the 3 periods of the reproductive cycle. Total RNA was extracted from ovary of Xupu geese at different ages. Fifteen cDNA sequencing libraries (5 pre-laying period samples, 5 egg-laying period samples, and 5 broody period samples) were prepared and sequenced on the Illumina Hiseq platform. More than 4.1×10^7 clean reads per sample were generated after filtering. The clean reads were characterized by more than 92% of Q30 with a GC content of approximately 50% (Table 1). In addition, more than 82% of clean reads were perfectly mapped to the reference goose genomes (ftp://ftp.ensembl.org/pub/release-101/fasta/anser_cygnoides/) to generate a read count value. All subsequent analyses were based on mapped reads and raw data were submitted to the NCBI database (SUB8312645).

Validation of RNA-Seq Data Using qPCR

Following RNA-seq analysis, 7 highly expressed DEGs were selected randomly for further validation with qRT-PCR (Table 2). qRT-PCR analysis data showed that most trends of upregulation or downregulation for the selected 7 genes corroborated with results from RNA-seq analysis (Figure 1). qRT-PCR findings validated the accuracy and reliability of RNA-seq analysis results.

DEGs in the Pre-laying Period, Egg-laying Period, or Broody Period

Total RNA was extracted from ovarian tissue of 3 important reproduction periods to give an overview of goose ovarian changes and allow for the exploration of the related gene and pathways of broodiness. A heatmap of DEGs (Figure 2A) and Pearson correlation coefficient of the samples (Figure 2B) demonstrated good sample repeatability in each group. Analysis using DESeq2 R package revealed 6,127 upregulated and 4,112 downregulated DEGs in T1 vs. T2 (Figure 2C), 521 upregulated and 803 downregulated DEGs in T1 vs. T3 (Figure 2D), and 3998 upregulated and 5712 downregulated DEGs

Table 1. Summary of Illumina RNA-seq data.

Group	Sample	Total reads	Clean reads	Total mapped Clean data* (Gb)	Q30 (%)	GC (%)	Total map Rate (%)
Pre-laying Period	T1_1	53724448	52649734	7.9	92.88	50.38	85.64
	T1_2	48537944	47388374	7.11	93.07	50.78	83.74
	T1_3	45525954	44780912	6.72	92.87	50.13	82.56
	T1_4	46500408	45719558	6.86	92.73	50.58	84.26
	T1_5	53724448	52649734	7.9	92.88	50.38	86.38
Egg-laying Period	T2_1	45357328	44660502	6.7	92.68	50.47	83.08
	T2_2	46630778	45276860	6.79	94.77	53.11	82.2
	T2_3	46595642	45170742	6.78	94.43	52.62	83.18
	T2_4	47682596	46355658	6.95	94.7	52.4	81.34
	T2_5	46931022	45638700	6.85	94.63	52.31	82.83
Broody Period	T3_1	43081800	41777300	6.27	93.62	51.94	85.06
	T3_2	43133282	41865106	6.28	93.55	54.13	84.84
	T3_3	45730386	44495388	6.67	93.37	51.73	84.13
	T3_4	42388562	41154010	6.17	93.56	51.72	84.84
	T3_5	46141102	44868082	6.73	93.28	51.71	84.51

*Clean data were obtained from raw data by removing reads containing adapter, ploy-N and low-quality reads.

Table 2. Validation of DGEs by qRT-PCR.

Gene name		Primers	Description	Product size (bp)
GCK	FP	CGGCACGCTCTACAAGC	glucokinase (hexokinase 4)	188
	RP	GCAAACCTCCCTCCTCCT		
ITGB2	FP	GGGCTCCTCCACATTTC	integrin 2C beta 2 (complement component 3	102
	RP	TTCAGATTGCTGCTCCTTT	receptor 3 and 4 subunit) 2C transcript variant X1	
LCP1	FP	CACAGAGGATGGCAGGA	lymphocyte cytosolic protein 1 (L-plastin)	129
	RP	ATCCCACCAATAGCACAGA		
MPEG1	FP	CAGAGGCCCCAAGGTTT	macrophage expressed 1	140
	RP	CATGTCGTGGTGGGTCA		
PTAFR	FP	GCACTGGGGCTTTGTCT	platelet activating factor receptor	144
	RP	GCTGACTTTGACCTGCCT		
STRA6	FP	GCAGGACAACACATTTCCC	stimulated by retinoic acid 6	128
	RP	GGCGTTTCACCAGCAAG		
SLA	FP	AGAGTGCCCTTCACTTGC	Src-like-adaptor	64
	RP	TTACCCCTCTGGTTGTCCT		
GAPDH	FP	TGGCATCCAAGGAGTAAGC	house-keeping gene for qRT-PCR	72
	RP	GGGCTCCAACAAAGGGT		

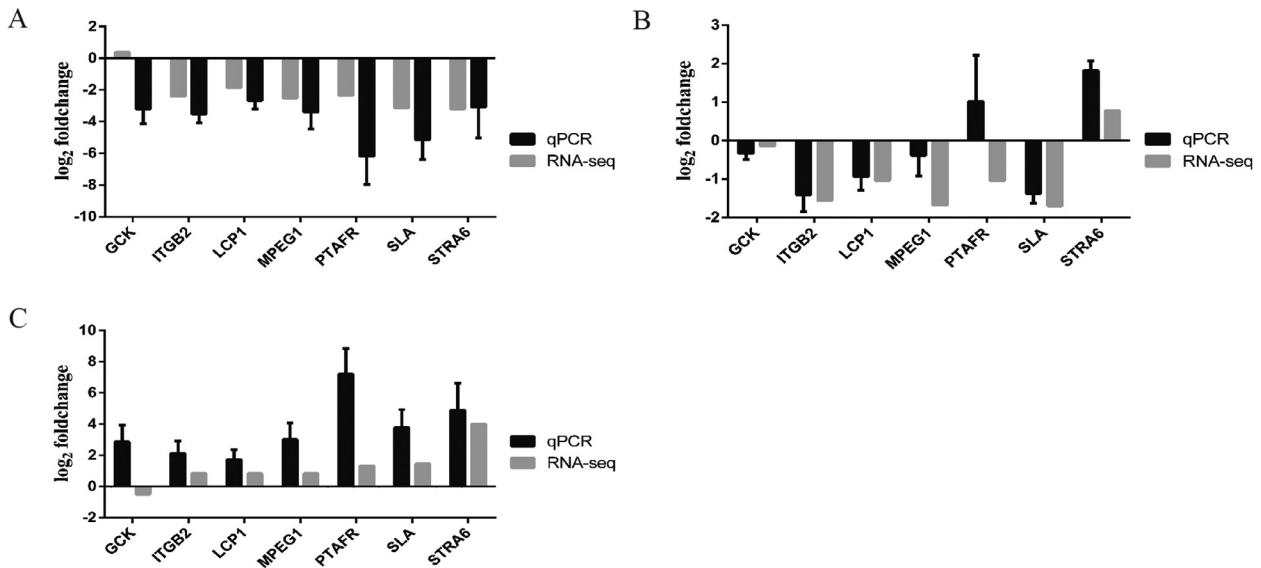Abbreviation: DEGs, differentially expressed genes; qRT-PCR, quantitative real-time PCR.

Figure 1. Validation of sequencing data by qPRC. Validation of the results for pre-laying period (T1), egg-laying period (T2) and broody period (T3). (A) T1 vs. T2; (B) T1 vs. T3; (C) T2 vs. T3. All data are presented as means ± SEM, x-axis individual genes whereas y-axis represents the fold change in expression determined by RNA-seq (gray bars) or qPCR (black bars). The representative genes are GCK (glucokinase), ITGB2 (integrin subunit beta 2), LCP1 (lymphocyte cytosolic protein 1), MPEG1 (macrophage expressed 1), PTAFR (platelet-activating factor receptor), SLA (Src-like-adaptor), STRA6 (stimulated by retinoic acid 6) and GAPDH (glyceraldehyde-3-phosphate dehydrogenase, house-keeping gene for qPCR).

inT2 vs. T3 (Figure 2E). A Venn diagram (Figure 2F) depicted common DEGs among T1, T2, and T3 periods. Of the 12,447 DEGs, 258 DEGs showed significant differences between the 3 groups (Supplementary material 1). These 258 DEGs are implicated in multiple physiological pathways, including inflammation, reproduction, mutual recognition and adhesion between cells, and formation of the cytoskeleton. Notably, expression patterns of *MRP126, serglycin, TXNIP,* and *FZD2* genes have, for the first time, been reported in the avian ovary from the pre-laying period to the broody period.

GO Enrichment Analysis of DEGs

We employed the GOseq R package for GO enrichment analysis of DEGs (Figure 3). In total, 69 GO terms were enriched in T1 vs. T2, including 25 molecular functions (**MF**) terms, 11 cell components (**CC**), and 33 biological processes (**BP**) terms (Supplementary material 2, P-value < 0.05). The top 10 significantly enriched GO terms in T1 vs. T2 were primarily associated with the regulation of synthesis and metabolism (8/10) and protein phosphorylation (2/10) (Table 3). Moreover, 59 GO terms were enriched between T2 vs. T3, including 36 BP terms, 5 CC terms, and 18 MF terms (Supplementary material 2, P-value < 0.05). The top 10 significantly enriched GO terms in T2 vs. T3 were implicated in protein phosphorylation (2/10), cell or biological adhesion (2/10), and regulation of multiple compound metabolic processes (6/10) (Table 3). Analysis of DEGs in T1 with T3 showed 79 enriched GO terms, including 48 BP terms, 13 CC terms, and 18 MF terms (Supplementary
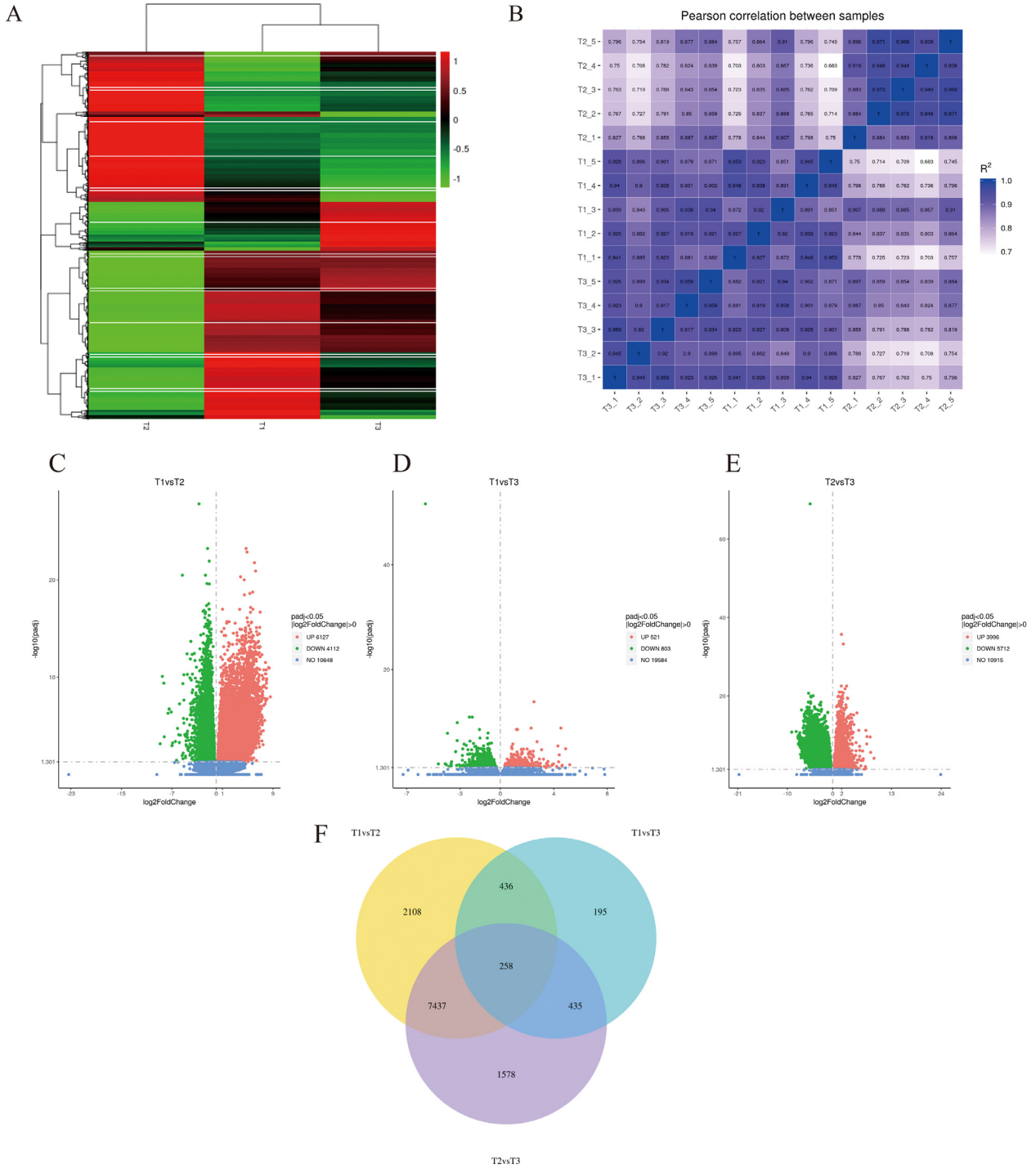
Figure 2. Differentially expressed genes from the three reproduction periods. (A) Heat maps of DEGs from ovaries during pre-egg period (T1), laying-egg period (T2) and broody period (T3). The read counts of each cellular mRNA were normalized by the sum of the total reads. Colors from white to red represent upregulated cellular genes; colors from white to green represent downregulated cellular genes. (B) Pearson correlation analysis of T1, T2, and T3 groups. Volcano plot of corrected *P* values as a function of weighted fold change for mRNAs in T1 vs. T2 (C); T1 vs. T3 (D); (C) T2 vs. T3 (E). The vertical dotted line delimits up- and downregulation. Red plots represent significant upregulated genes and green plots represent significant downregulated genes (|log2-fold change|≥0, corrected *P* < 0.05). (F) A Venn diagram showed the relationships among T1, T2, and T3 groups of DEGs. A total of 258 DEGs were identified in all 3 groups. Abbreviation: DEGs, differentially expressed genes.

material 2, *P*-value < 0.05). The top 10 significantly enriched GO terms were implicated in ATP hydrolysis coupled-related compounds transport (4/10), transmembrane transport (3/10), and others (3/10) (Table 3). Of note, 39 GO terms were significantly enriched in both T1 vs. T2 and T2 vs. T3 and were mainly involved in the regulation of signaling or biosynthetic process (18/39), cellular components (4/39), protein polymerization (5/39), nucleic acid synthesis, and transcription (8/39), and others (4/39). These data are in support of the view that these GO terms may play critical roles in the entire ovulation cycle.
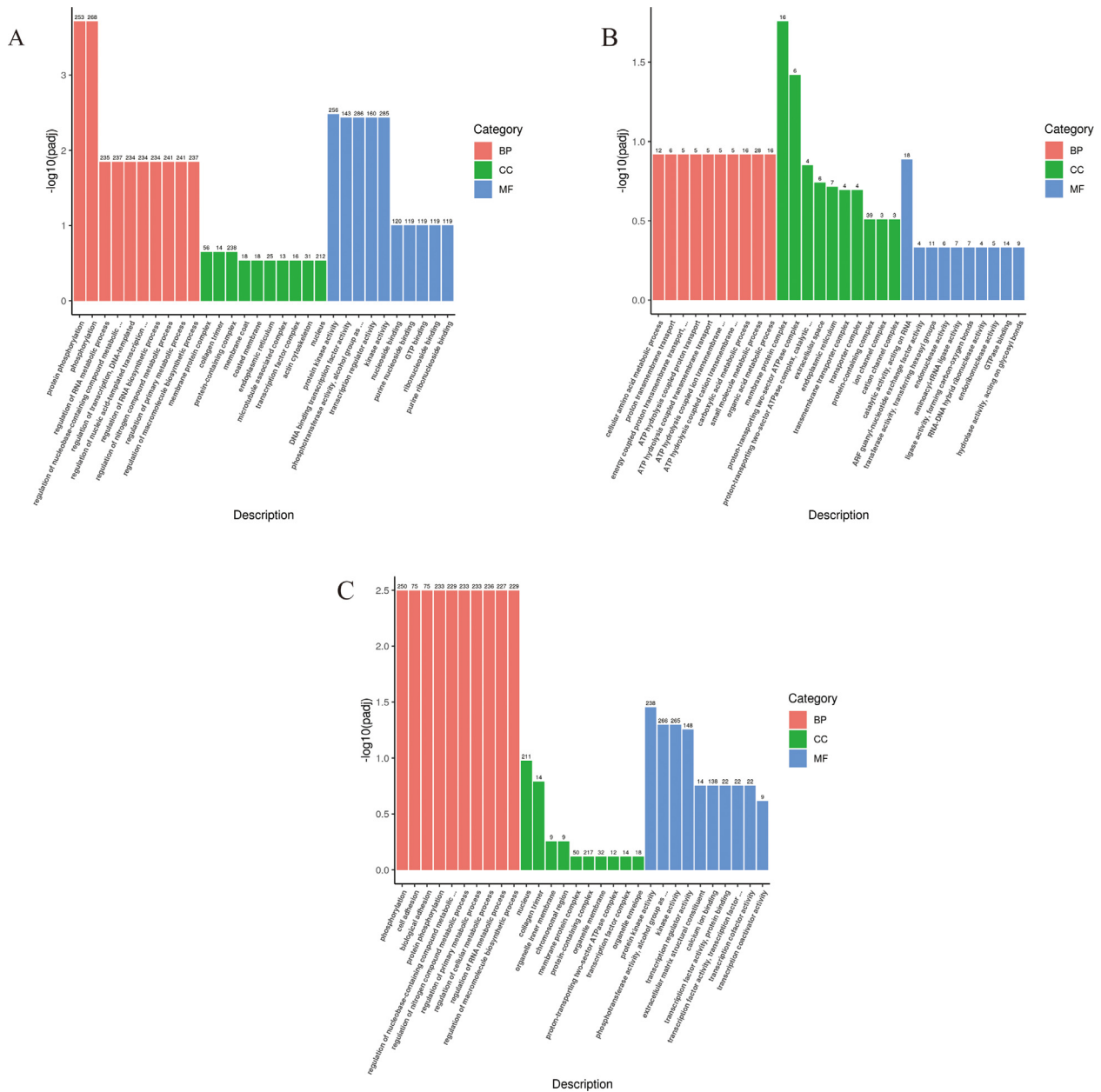
Figure 3. GO terms enrichment analysis of DEGs in ovaries. Histogram charts show the top 30 significantly enriched GO terms of T1 vs. T2 (A), T1 vs. T3 (B), T2 vs. T3 (C), which are classified as biological process (BP, red bar), cellular component (CC, green bar) and molecular function (MF, blue bar). Abbreviations: DEGs, differentially expressed genes; GO, gene ontology.

KEGG Pathway Enrichment Analysis of DEGs

Functional classification of the DEGs using KEGG pathway enrichment analysis (Figure 4) demonstrated that the DEGs were associated with 18 pathways in T1 vs. T2, 11 pathways in T1 vs. T3, and 5 pathways in T2 vs. T3 (Supplementary material 3). The top 5 KEGG pathways in T1 vs. T2 were focal adhesion (gga04510), regulation of actin cytoskeleton (gga04810), salmonella infection (gga05132), protein processing in the endoplasmic reticulum (gga04141), and influenza A (gga05164) (Table 4). The top 5 pathways in T1 vs. T3 were lysosome (gga04142), N-glycan biosynthesis (gga00510), spliceosome (gga03040),

types of N-glycan biosynthesis (gga00513), and sphingolipid metabolism (gga00600) (Table 4). Moreover, the top 5 pathways in T2 relative to T3 were focal adhesion (gga04510), ECM-receptor interaction (gga04512), N-glycan biosynthesis (gga00510), TGF-beta signaling pathway (gga04350), and endocytosis (gga04144) (Table 4).

Comparative analysis of enriched KEGG pathways in the three periods revealed that three common pathways, including focal adhesion (gga04510), ECM-receptor interaction (gga04512), and N-glycan biosynthesis (gga00510) were enriched between the groups. Taken together, these findings help define the potential central role of these enriched pathways in the entire ovulation cycle.

Table 3. Top 10 enriched GO terms in T1 vs. T2, T1 vs. T3 and T2 vs. T3.

| Comparison between two groups	Category	GO ID	Description	GeneRatio	BgRatio	P value	Count	Up	Down
T1	BP	GO:0006468	protein phosphorylation	253/2434	407/4798	8.19E-07	253	105	148
vs.	BP	GO:0016310	phosphorylation	268/2434	434/4798	8.48E-07	268	113	155
T2	MF	GO:0004672	protein kinase activity	256/4089	414/7920	1.12E-05	256	106	150
	MF	GO:0003700	DNA binding transcription factor activity	143/4089	221/7920	4.66E-05	143	54	89
	MF	GO:0016773	phosphotransferase activity, alcohol group as acceptor	286/4089	474/7920	5.21E-05	286	114	172
	MF	GO:0140110	transcription regulator activity	160/4089	251/7920	5.54E-05	160	60	100
	MF	GO:0016301	kinase activity	285/4089	473/7920	6.20E-05	285	116	169
	BP	GO:0051252	regulation of RNA metabolic process	235/2434	398/4798	0.000311	235	102	133
	BP	GO:0019219	regulation of nucleobase-containing compound metabolic process	237/2434	402/4798	0.000333	237	104	133
	BP	GO:0006355	regulation of transcription, DNA-templated	234/2434	397/4798	0.000371	234	101	133
T1	CC	GO:0098796	membrane protein complex	16/186	88/2755	0.000188	16	5	11
vs.	MF	GO:0140098	catalytic activity, acting on RNA	18/585	104/7917	0.000544	18	2	16
T3	CC	GO:0016469	proton-transporting two-sector ATPase complex	6/186	18/2755	0.000818	6	0	6
	BP	GO:0006520	cellular amino acid metabolic process	12/340	63/4790	0.001322	12	1	11
	BP	GO:1902600	proton transmembrane transport	6/340	20/4790	0.002019	6	0	6
	BP	GO:0015988	energy coupled proton transmembrane transport, against electrochemical gradient	5/340	15/4790	0.002899	5	0	5
	BP	GO:0015991	ATP hydrolysis coupled proton transport	5/340	15/4790	0.002899	5	0	5
	BP	GO:0090662	ATP hydrolysis coupled transmembrane transport	5/340	15/4790	0.002899	5	0	5
	BP	GO:0099131	ATP hydrolysis coupled ion transmembrane transport	5/340	15/4790	0.002899	5	0	5
	BP	GO:0099132	ATP hydrolysis coupled cation transmembrane transport	5/340	15/4790	0.002899	5	0	5
T2	BP	GO:0016310	phosphorylation	250/2298	433/4775	1.67E-05	250	142	108
vs.	BP	GO:0007155	cell adhesion	75/2298	112/4775	3.63E-05	75	44	31
T3	BP	GO:0022610	biological adhesion	75/2298	112/4775	3.63E-05	75	44	31
	BP	GO:0006468	protein phosphorylation	233/2298	406/4775	5.78E-05	233	134	99
	BP	GO:0019219	regulation of nucleobase-containing compound metabolic process	229/2298	400/4775	8.33E-05	229	113	116
	BP	GO:0051171	regulation of nitrogen compound metabolic process	233/2298	408/4775	8.96E-05	233	114	119
	BP	GO:0080090	regulation of primary metabolic process	233/2298	408/4775	8.96E-05	233	114	119
	BP	GO:0031323	regulation of cellular metabolic process	236/2298	414/4775	9.45E-05	236	115	121
	BP	GO:0051252	regulation of RNA metabolic process	227/2298	397/4775	9.99E-05	227	113	114
	BP	GO:0010556	regulation of macromolecule biosynthetic process	229/2298	401/4775	0.000104	229	114	115

Abbreviation: GO, gene ontology.
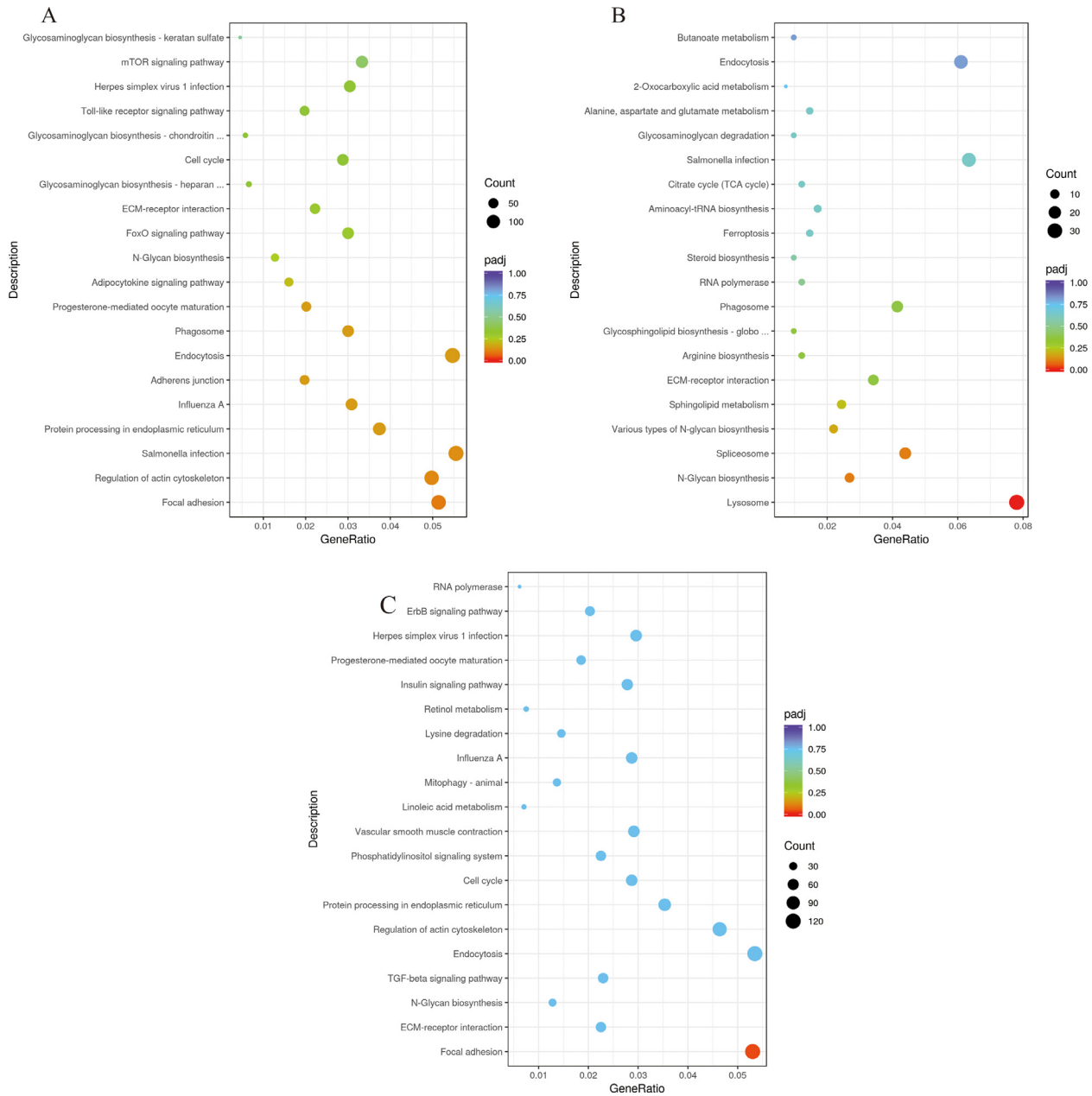
Figure 4. KEGG pathway enrichment analysis of DEGs in ovaries. Bubble charts represent the top 20 significantly enriched KEGG pathways of T1 vs. T2 (A), T1 vs. T3 (B), T2 vs. T3 (C). Size of each circle represents the number of DEGs in each pathway (larger circles represent more DEGs) and the color represents the *P* value of each pathway. Abbreviations: DEGs, differentially expressed genes; KEGG, Kyoto Encyclopedia of Genes and Genomes.

DISCUSSION

Unlike in mammals, goose follicles do not undergo atresia. This is the reason why avian species have long-term continuous egg production, which is influenced by ovarian follicle development and ovulation. Although Xupu goose (*Anser cygnoides domesticus*) is a nationally and commercially important farm animal in Hunan Province, its strong broody and poor egg-laying performance are limiting its economic value in the farm industry. In this study, ovary tissues were collected from Xupu gooses in the pre-laying period, laying period, and broody period. The total RNA was sequenced on the Illumina MiSeq platform to reveal differentially

expressed gene transcripts in the ovary of Xupu geese from the pre-laying period to the broody period. We reported transcriptome changes of ovarian tissue in the entire reproduction period of Xupu geese. KEGG and GO analyses further revealed the key genes and pathways implicated in the laying cycle and brooding of Xupu geese. Analysis showed, 258 genes are significantly differentially expressed in T1 vs. T2, T1 vs. T3, and T2 vs. T3, and are implicated in inflammation, reproduction, mutual recognition and adhesion between cells, and the establishment of the cytoskeleton.

The broody behavior of goose is a significant aspect of their reproduction. It influences egg production with the degeneration of follicles. Mounting evidence has shown

Table 4. Top 5 enriched KEGG pathways in T1 vs. T2, T1 vs. T3 and T2 vs. T3.

Comparison between two groups	KEGG ID	Description	P value	P adj	Count	Up	Down
T1	gga04510	Focal adhesion	0.000662	0.099952	125	22	103
vs.	gga04810	Regulation of actin cytoskeleton	0.001571	0.118588	121	29	92
T2	gga05132	Salmonella infection	0.002563	0.129018	135	41	94
	gga04141	Protein processing in endoplasmic reticulum	0.005158	0.150095	91	26	65
	gga05164	Influenza A	0.005641	0.150095	75	14	61
T1	gga04142	Lysosome	9.53E-10	1.34E-07	32	1	31
vs.	gga00510	N-Glycan biosynthesis	0.001436	0.101227	11	2	9
T3	gga03040	Spliceosome	0.002174	0.102192	18	4	14
	gga00513	Various types of N-glycan biosynthesis	0.004959	0.174818	9	2	7
	gga00600	Sphingolipid metabolism	0.007867	0.221839	10	2	8
T2	gga04510	Focal adhesion	0.000213	0.032159	120	93	27
vs.	gga04512	ECM-receptor interaction	0.020819	0.757549	51	40	11
T3	gga00510	N-Glycan biosynthesis	0.02695	0.757549	29	14	15
	gga04350	TGF-beta signaling pathway	0.036209	0.757549	52	37	15
	gga04144	Endocytosis	0.03976	0.757549	121	63	58

Abbreviation: KEGG, Kyoto Encyclopedia of Genes and Genomes.

that the degeneration of follicles is associated with autophagy, apoptosis, and homeostasis imbalance (Yu et al., 2016b). Autophagy is implicated in both cell survival and cell death. Herein, we found that the expression of several autophagy-related genes, including *AMBRA1, ATGs, DRAM1, MAP1LC3A, SOGA1, UVRAG, VPS13A, VPS13C,* and *WDFY3* were altered in the ovary at different stages. In support of our findings, Yu et al. (2016c) also revealed that the expression of some autophagy relative genes, including *BECN1, TP63,* and *ATGs,* were alerted in the broody follicles. Autophagy is a multistep process highly regulated by a number of the conserved autophagy-related genes (**ATGs**) (Liu et al., 2010). Emerging evidence indicates that *ATG* genes are crucial in autophagosome formation and autophagy regulation, and are also associated with several key pathological and physiological processes (Levine and Kroemer, 2008). In particular, *ATG4B*, a mammalian homologue of yeast Atg4, has been implicated in the processing of LC3. Its protein and mRNA expressions were ubiquitous in rat tissues (Yoshimura et al., 2006). Our results showed lower mRNA relative expression of *Atg4B* significantly in the laying period as compared with the pre-laying period and broody period. Moreover, a few DEGs and GO terms were associated with apoptosis, a form of programmed cell death, or "cellular suicide." All peptidases of the C14 family have a strict requirement for the amino acid in P1. The apoptosis cascade, predominant in animal cells, is primarily regulated by the caspases. In this study, we revealed significant alteration of the relative expression of some genes belonging to the Peptidase C14 family, in these 3 periods. They included *CASP10, CASP6, CASP7, CFLAR, CASP9,* and *CASP8.* Of note, the mRNA relative expression of *CASP10, CASP6* and *CASP7* significantly increased in the laying period as compared with the pre-laying period and broody period. *CASP6* is traditionally recognized as an crucial molecule in programmed cell apoptosis, it cleaves the nuclear structural protein NuMA (nuclear mitotic apparatus protein) and the lamin A/C proteins and induces nuclear shrinkage

and fragmentation (Li and Yuan, 2008). Indeed, *CASP6* exerts crucial regulatory effects on non-apoptotic cellular events, such as modification of cell cycle entry (Richards et al., 2008). Caspase-10, a close homolog of caspase-8, is a highly conserved caspase throughout evolution (Eckhart et al., 2008). It is currently assumed that caspase-8 and caspase-10 have redundant functions in cell death signaling, though the potential function of caspase-10 as a substitute for caspase-8 is controversial (Fischer et al., 2006). Caspase-3 is the most important executioner caspase, activated by both intrinsic and extrinsic pathways (Seervi and Xue, 2015).

In the recent past, differences in the mRNA levels of *CASP3* among primordial, primary, and secondary follicles, and the magnitude were revealed, though they varied according to species (duck and goose) and the stages of development (Hu et al., 2021). Contrary to previous works, *CASP3* expression differed in the 3 stages of our experiment, but the difference was not statistically significant. These results suggest a role for apoptosis and autophagy in different reproductive stages, but warrant further exploration of the specific role and underlying mechanism.

Of note, this is the first report on the expression pattern of *MRP126, serglycin, TXNIP,* and *FZD2* genes in the avian ovary. Bukovsky and Presl (1979) reported the association between the immune system and the regulation of ovulation. Mounting reports show that several mediators of LH-induced signaling cascades are associated with inflammation, and the process leading to ovulation and that of the inflammatory response are similar (Duffy et al., 2019; Ernst et al., 2020). In the present study, *MRP126* was significantly upregulated in the pre-laying period vs. egg-laying period and significantly downregulated in the egg-laying vs. broody period. We also reported a higher relative expression of *MRP126* in the broody period as compared with that in the pre-laying period. MRP126 protein is a co-orthologue of calgranulin, expressed solely in birds and reptiles (Loes et al., 2018). High expression levels of MRP126 protein have previously been reported in chicken tissues, including

heterophils (avian counterparts of mammalian neutrophils), caecum, and macrophages, following bacteria exposure (Matulova et al., 2013; Rychlik et al., 2014). A similar pattern of expression of MRP126 and calgranulin is observed when birds or mammals are infected by bacteria. Although there is no previous data on MRP126 expression in the avian ovary, studies reported expression profiles of calgranulin protein in the mammalian ovary. Mammals express 3 distinct members of the calgranulins family, including S100A8 (calgranulin A), S100A9 (calgranulin B), and S100A12 (calgranulin C) (Bozzi and Nolan, 2020). S100A8 is primarily expressed in oocytes within cysts/plasmodia where it induces oocytes or ovarian somatic cells to form primordial follicles (Teng et al., 2015). S100A9 forms a heterodimer with S100A8 under calcium (Teigelkamp et al., 1991) and the resultant complex contributes to inflammatory processes (Hessian et al., 1993). mRNA expression of S100A9 is upregulated in both granulosa cells and residual ovarian cells 6 h after hCG injection and then sharply declines by 12 h post-hCG injection. In situ hybridization analysis shows that S100A9 mRNA is expressed predominantly in cells located in the interstitial and stroma layer of preovulatory ovaries. However, data on the specific expression pattern of S100A9 in different parts of the ovary is scanty. Besides, S100A9 upregulation demonstrates its significant role in leukocyte trafficking during inflammatory responses of ovulation (Jo et al., 2004). This is the first study to report *MRP126* expression profile in avian ovary, and implicate *MRP126* in ovulation induced inflammatory response.

Serglycin was first reported as a secretory product of a rat yolk sac tumor (Oldberg et al., 1981). Herein, we the first group to report the *serglycin* mRNA profile in ovarian tissue of goose during the whole ovulation cycle. *Serglycin* expression during the pre-laying period was significantly lower, as compared with its expression in the other 2 periods. Besides, *serglycin* was significantly upregulated during the egg-laying period and then significantly downregulated during the broody period. Several lines of evidence had revealed that serglycin is primarily expressed in cells with hematopoietic lineage, including neutrophils, lymphocytes, monocytes, macrophages, and mast cells (Elliott et al., 1993; Niemann et al., 2004). It also interacts with various inflammatory mediators (Kolset and Tveit, 2008). Serglycin has further been implicated in uterine decidual function (Keith Ho et al., 2001), extravasation of peripheral blood natural killer cells into the endometrium (Santoni et al., 2008), and signaling within the decidua, or between the placenta and the decidua (Schick, 2010). Ferrazza (Ferrazza et al., 2017) explored the protein expression profile of bovine follicular fluid at different development stages and reported serglycin upregulation in early follicular development and a negative correlation of serglycin expression level with progesterone concentration in follicular fluid (Ferrazza et al., 2017). The expression pattern of *serglycin* supports the view that it plays a role in the ovulation-induced inflammatory response.

In addition, the functions of the ovary are influenced by metabolism. There is previous evidence that obesity, insulin resistance, oxidative stress, and reproductive hormone imbalance induce ovarian dysfunction (Robker, 2008; Gu et al., 2015). Our analysis showed that *TXNIP* was highly expressed in the 3 periods, in particular, *TXNIP* was significantly upregulated in the egg-laying and broody period as compared with the pre-laying period. TXNIP (thioredoxin-interacting protein) is a redox-sensitive signaling protein implicated in glucose metabolism (Patwari et al., 2006), and it is associated with insulin resistance and insulin secretion (Wu et al., 2014). Studies have reported high expression TXNIP in cumulus cells, oocytes, and granulosa cells of several species (Lee et al., 2013; Salhab et al., 2013). Obesity leads to downregulation of TXNIP expression in metaphase II of oocytes compared with expression levels of the normal group, which may reduce development and quality of oocyte (Ruebel et al., 2017). In addition, Chutkow (Chutkow et al., 2008) revealed that TXNIP modulated hepatic glucose production and global glucose homeostasis (Chutkow et al., 2008), whereas Parikh (Parikh et al., 2007) found that low TXNIP levels improved glucose uptake in skeletal muscle (Parikh et al., 2007). These data suggest that TNXIP plays multiple roles in the process of oocyte maturation. Our study is the first to explore the *TNXIP* mRNA profile in the ovary of a goose during the reproductive cycle, and future research direction will be to explore the specific function of TNXIP in the ovary.

The Wnt pathway is a conserved signaling pathway implicated in the regulation of ovarian development and function. Wnt signaling components are expressed in the human ovary from early to mid-gestation. Of note, canonical Wnt signaling is only observed in oocytes of primordial follicles (Bothun and Woods, 2019). *FZD2* is linked to the Wnt pathway. In this study, the relative expression of *FZD2* was at its peak during the egg-laying period and then declined during the broody period. FZD2 was first reported by (Zhao et al., 1995) in developing ovaries. In the same study, high expression levels of the frizzled receptor were reported throughout ovary development, an implication that Wnt-signaling was mediated via the non-canonical pathway. The profiles of Wnt signaling components have previously been explored in the human ovary from development to adulthood. As depicted by the germ cell nests, FZD2 was expressed at all time-points of ovarian development but strictly in low cytoplasmic levels in adult tissue (Bothun and Woods, 2019). In the past decade, Wang (Wang et al., 2010) explored the expression pattern of FZD2 in mouse ovaries during the oestrous cycle and reported the highest FZD2 mRNA and protein levels in murine oocytes and granulosa cells during the proestrus stage which significantly decreased from oestrus to diestrus stages. Additionally, the expression profiles of FZD2 in both human and mouse ovary tissues demonstrated that FZD2 was involved in the regulation of follicular growth, oocyte maturation, and luteinization in mammals. This is the first study to report the expression

pattern of *FZD2* in the avian ovary from the pre-laying period to the broody period. However, the role of *FZD2* in the development and regulation of ovulation should be explored further.

In summary, this study reports on the entire profile of transcriptome changes in ovaries from the pre-laying period to the broody period. Candidate genes implicated in the whole cycle have also been identified. These findings demonstrate a role for inflammation, reproduction, mutual recognition and adhesion between cells, and the establishment of the cytoskeleton, in the ovarian cycle changes. These data will provide valuable information to improve Xupu goose breeding with low nestability in the future.

ACKNOWLEDGMENTS

DISCLOSURES

The authors declare no conflict of interest.

SUPPLEMENTARY MATERIALS

Supplementary material associated with this article can be found, in the online version, at doi:10.1016/j.psj.2021.101403.

REFERENCES

Bothun, A. M., and D. C. Woods. 2019. Dynamics of WNT signaling components in the human ovary from development to adulthood. Histochem. Cell. Biol. 151:115–123.

Bozzi, A. T., and E. M. Nolan. 2020. Avian MRP126 restricts microbial growth through Ca(II)-Dependent Zn(II) sequestration. Biochemistry 59:802–817.

Bukovsky, A., and J. Presl. 1979. Ovarian function and the immune system. Med. Hypotheses. 5:415–436.

Chutkow, W. A., P. Patwari, J. Yoshioka, and R. T. Lee. 2008. Thioredoxin-interacting protein (Txnip) is a critical regulator of hepatic glucose production. J. Biol. Chem. 283:2397–2406.

Dai, Q. Z., Q. Lin, and G. T. Jiang. 2016. Phylogenetic studies of four Anser cygnoides (Anserini: Anserinae) in Hunan province of China based on complete mitochondrial DNA sequences. Mitochondrial. DNA. A. DNA. Mapp. Seq. Anal. 27:2464–2465.

Ding, N., Q. Han, X. Z. Zhao, Q. Li, J. Li, H. F. Zhang, G. L. Gao, Y. Luo, Y. H. Xie, J. Su, and Q. G. Wang. 2015. Differential gene expression in pre-laying and laying period ovaries of Sichuan White geese (Anser cygnoides). Genet. Mol. Res. 14:6773–6785.

Duffy, D. M., C. Ko, M. Jo, M. Brannstrom, and T. E. Curry. 2019. Ovulation: parallels with inflammatory processes. Endocr. Rev. 40:369–416.

Eckhart, L., C. Ballaun, M. Hermann, J. L. VandeBerg, W. Sipos, A. Uthman, H. Fischer, and E. Tschachler. 2008. Identification of novel mammalian caspases reveals an important role of gene loss in shaping the human caspase repertoire. Mol. Biol. Evol. 25:831–841.

Elliott, J. F., C. L. Miller, B. Pohajdak, D. Talbot, C. D. Helgason, R. C. Bleackley, and V. Paetkau. 1993. Induction of a proteoglycan core protein mRNA in mouse T lymphocytes. Mol. Immunol. 30:749–754.

Ernst, E. H., M. Amoushahi, A. S. Sørensen, T. W. Kragstrup, E. Ernst, and K. Lykke-Hartmann. 2020. Distinct expression patterns of TLR transcripts in human oocytes and granulosa cells from primordial and primary follicles. J. Reprod. Immunol. 140:103125.

Everaert, C., M. Luypaert, J. L. V. Maag, Q. X. Cheng, and P. Mestdagh. 2017. Benchmarking of RNA-sequencing analysis workflows using whole-transcriptome RT-qPCR expression data. Sci. Rep. 7:1588.

Ferrazza, R. A., H. D. M. Garcia, E. Schmidt, M. Mihm Carmichael, F. F. Souza, R. Burchmore, R. Sartori, P. D. Eckersall, and J. C. P. Ferreira. 2017. Quantitative proteomic profiling of bovine follicular fluid during follicle development. Biol. Reprod. 97:835–849.

Fischer, U., C. Stroh, and K. Schulze-Osthoff. 2006. Unique and overlapping substrate specificities of caspase-8 and caspase-10. Oncogene 25:152–159.

Gao, G., Q. Li, X. Zhao, N. Ding, Q. Han, J. Su, and Q. Wang. 2015. Transcriptome profiling of the hypothalamus during prelaying and laying periods in Sichuan white geese (Anser cygnoides). Anim. Sci. J. 86:800–805.

Geng, A. L., S. F. Xu, Y. Zhang, J. Zhang, Q. Chu, and H. G. Liu. 2014. Effects of photoperiod on broodiness, egg-laying and endocrine responses in native laying hens. Br. Poult. Sci. 55:264–269.

Gu, L., H. Liu, X. Gu, C. Boots, K. H. Moley, and Q. Wang. 2015. Metabolic control of oocyte development: linking maternal nutrition and reproductive outcomes. Cell. Mol. Life Sci. 72:251–271.

Gumułka, M., A. Hrabia, N. Avital-Cohen, K. Andres, and I. Rozenboim. 2020. The effect of parachlorophenylalanine treatment on the activity of gonadal and lactotrophic axes in native Polish crested chickens stimulated to broodiness. Poult. Sci. 99:2708–2717.

Hessian, P. A., J. Edgeworth, and N. Hogg. 1993. MRP-8 and MRP-14, two abundant Ca(2+)-binding proteins of neutrophils and monocytes. J. Leukoc. Biol. Suppl. 53:197–204.

Hu, S., M. Zhu, J. Wang, L. Li, H. He, B. Hu, J. Hu, and L. Xia. 2021. Histomorphology and gene expression profiles during early ovarian folliculogenesis in duck and goose. Poult. Sci. 100:1098–1108.

Jo, M., M. C. Gieske, C. E. Payne, S. E. Wheeler-Price, J. B. Gieske, I. V. Ignatius, T. E. Curry Jr., and C. Ko. 2004. Development and application of a rat ovarian gene expression database. Endocrinology 145:5384–5396.

Kang, B., J. R. Guo, H. M. Yang, R. J. Zhou, J. X. Liu, S. Z. Li, and C. Y. Dong. 2009. Differential expression profiling of ovarian genes in prelaying and laying geese. Poult. Sci. 88:1975–1983.

Ho, Keith, H. C., K. E. McGrath, K. C. Brodbeck, J. Palis, and B. P. Schick. 2001. Serglycin proteoglycan synthesis in the murine uterine decidua and early embryo. Biol. Reprod. 64:1667–1676.

Kolset, S. O., and H. Tveit. 2008. Serglycin−structure and biology. Cell. Mol. Life Sci. 65:1073–1085.

Lee, S. Y., H. S. Lee, E. Y. Kim, J. J. Ko, T. K. Yoon, W. S. Lee, and K. A. Lee. 2013. Thioredoxin-interacting protein regulates glucose metabolism and affects cytoplasmic streaming in mouse oocytes. Plos One 8:e70708.

Levine, B., and G. Kroemer. 2008. Autophagy in the pathogenesis of disease. Cell 132:27–42.

Li, J., and J. Yuan. 2008. Caspases in apoptosis and beyond. Oncogene 27:6194–6206.

Liu, B., Y. Cheng, Q. Liu, J. K. Bao, and J. M. Yang. 2010. Autophagic pathways as new targets for cancer drug development. Acta Pharmacol. Sin. 31:1154–1164.

Liu, H., J. Wang, L. Li, C. Han, H. He, and H. Xu. 2018. Transcriptome analysis revealed the possible regulatory pathways initiating female geese broodiness within the hypothalamic-pituitary-gonadal axis. Plos One 13:e0191213.

Loes, A. N., J. T. Bridgham, and M. J. Harms. 2018. Coevolution of the toll-like receptor 4 complex with calgranulins and lipopolysaccharide. Front. Immunol. 9:304.

Luan, X., D. Liu, Z. Cao, L. Luo, M. Liu, M. Gao, and X. Zhang. 2014. Transcriptome profiling identifies differentially expressed genes in Huoyan goose ovaries between the laying period and ceased period. Plos One 9:e113211.

Marsden, S. J., L. M. Lucas, and S. P. Wilson. 1966. The influence of daylength and environment on reproduction, broodiness, and mortality of turkeys. Poult. Sci. 45:668–675.

Matulova, M., K. Varmuzova, F. Sisak, H. Havlickova, V. Babak, K. Stejskal, Z. Zdrahal, and I. Rychlik. 2013. Chicken innate immune response to oral infection with Salmonella enterica serovar Enteritidis. Vet. Res. 44:37.

Niemann, C. U., J. B. Cowland, P. Klausen, J. Askaa, J. Calafat, and N. Borregaard. 2004. Localization of serglycin in human neutrophil granulocytes and their precursors. J. Leukoc. Biol. 76:406–415.

Oldberg, A., E. G. Hayman, and E. Ruoslahti. 1981. Isolation of a chondroitin sulfate proteoglycan from a rat yolk sac tumor and immunochemical demonstration of its cell surface localization. J. Biol. Chem. 256:10847–10852.

Onagbesan, O., V. Bruggeman, and E. Decuypere. 2009. Intra-ovarian growth factors regulating ovarian function in avian species: a review. Anim. Reprod. Sci. 111:121–140.

Parikh, H., E. Carlsson, W. A. Chutkow, L. E. Johansson, H. Storgaard, P. Poulsen, R. Saxena, C. Ladd, P. C. Schulze, M. J. Mazzini, C. B. Jensen, A. Krook, M. Björnholm, H. Tornqvist, J. R. Zierath, M. Ridderstråle, D. Altshuler, R. T. Lee, A. Vaag, L. C. Groop, and V. K. Mootha. 2007. TXNIP regulates peripheral glucose metabolism in humans. PLoS Med 4:e158.

Patwari, P., L. J. Higgins, W. A. Chutkow, J. Yoshioka, and R. T. Lee. 2006. The interaction of thioredoxin with Txnip. Evidence for formation of a mixed disulfide by disulfide exchange. J. Biol. Chem. 281:21884–21891.

Richards, S., C. Watanabe, L. Santos, A. Craxton, and E. A. Clark. 2008. Regulation of B-cell entry into the cell cycle. Immunol. Rev. 224:183–200.

Robker, R. L. 2008. Evidence that obesity alters the quality of oocytes and embryos. Pathophysiology 15:115–121.

Romanov, M. N., R. T. Talbot, P. W. Wilson, and P. J. Sharp. 2002. Genetic control of incubation behavior in the domestic hen. Poult. Sci. 81:928–931.

Ruebel, M. L., M. Cotter, C. R. Sims, D. M. Moutos, T. M. Badger, M. A. Cleves, K. Shankar, and A. Andres. 2017. Obesity modulates inflammation and lipid metabolism oocyte gene expression: a single-cell transcriptome perspective. J. Clin. Endocrinol. Metab. 102:2029–2038.

Rychlik, I., M. Elsheimer-Matulova, and K. Kyrova. 2014. Gene expression in the chicken caecum in response to infections with non-typhoid Salmonella. Vet. Res. 45:119.

Salhab, M., S. Dhorne-Pollet, S. Auclair, C. Guyader-Joly, D. Brisard, R. Dalbies-Tran, J. Dupont, C. Ponsart, P. Mermillod, and S. Uzbekova. 2013. In vitro maturation of oocytes alters gene expression and signaling pathways in bovine cumulus cells. Mol. Reprod. Dev. 80:166–182.

Santoni, A., C. Carlino, H. Stabile, and A. Gismondi. 2008. Mechanisms underlying recruitment and accumulation of decidual NK cells in uterus during pregnancy. Am. J. Reprod. Immunol. 59:417–424.

Schick, B. P. 2010. Serglycin proteoglycan deletion in mouse platelets: physiological effects and their implications for platelet contributions to thrombosis, inflammation, atherosclerosis, and metastasis. Prog. Mol. Biol. Transl. Sci. 93:235–287.

Seervi, M., and D. Xue. 2015. Mitochondrial cell death pathways in caenorhabiditis elegans. Curr. Top. Dev. Biol. 114:43–65.

Sharp, P. J., M. C. MacNamee, R. T. Talbot, R. J. Sterling, and T. R. Hall. 1984. Aspects of the neuroendocrine control of ovulation and broodiness in the domestic hen. J. Exp. Zool. 232:475–483.

Teigelkamp, S., R. S. Bhardwaj, J. Roth, G. Meinardus-Hager, M. Karas, and C. Sorg. 1991. Calcium-dependent complex assembly of the myeloic differentiation proteins MRP-8 and MRP-14. J. Biol. Chem. 266:13462–13467.

Teng, Z., C. Wang, Y. Wang, K. Huang, X. Xiang, W. Niu, L. Feng, L. Zhao, H. Yan, H. Zhang, and G. Xia. 2015. S100A8, an oocyte-specific chemokine, directs the migration of ovarian somatic cells during mouse primordial follicle assembly. J. Cell. Physiol. 230:2998–3008.

Thomason, D. M., A. T. Leighton Jr., and J. P. Mason Jr.. 1976. A study of certain environmental factors and mineral chelation on the reproductive performance of young and yearling turkey hens. Poult. Sci. 55:1343–1355.

Wang, S. B., B. S. Xing, L. Yi, W. Wang, and Y. X. Xu. 2010. Expression of Frizzled 2 in the mouse ovary during oestrous cycle. J. Anim. Physiol. Anim. Nutr. 94:437–445.

Wu, J., Y. Wu, X. Zhang, S. Li, D. Lu, S. Li, G. Yang, and D. Liu. 2014. Elevated serum thioredoxin-interacting protein in women with polycystic ovary syndrome is associated with insulin resistance. Clin. Endocrinol. (Oxf.). 80:538–544.

Xu, Q., W. Zhao, Y. Chen, Y. Tong, G. Rong, Z. Huang, Y. Zhang, G. Chang, X. Wu, and G. Chen. 2013. Transcriptome profiling of the goose (Anser cygnoides) ovaries identify laying and broodiness phenotypes. Plos One 8:e55496.

Yao, Y., Y. Z. Yang, T. T. Gu, Z. F. Cao, W. M. Zhao, H. R. Qin, Q. Xu, and G. H. Chen. 2019. Comparison of the broody behavior characteristics of different breeds of geese. Poult. Sci. 98:5226–5233.

Ye, P., K. Ge, M. Li, L. Yang, S. Jin, C. Zhang, X. Chen, and Z. Geng. 2019. Egg-laying and brooding stage-specific hormonal response and transcriptional regulation in pituitary of Muscovy duck (Cairina moschata). Poult. Sci. 98:5287–5296.

Yoshimura, K., M. Shibata, M. Koike, K. Gotoh, M. Fukaya, M. Watanabe, and Y. Uchiyama. 2006. Effects of RNA interference of Atg4B on the limited proteolysis of LC3 in PC12 cells and expression of Atg4B in various rat tissues. Autophagy 2:200–208.

Yu, J., K. He, T. Ren, Y. Lou, and A. Zhao. 2016a. High-throughput sequencing reveals differential expression of miRNAs in prehierarchal follicles of laying and brooding geese. Physiol. Genomics 48:455–463.

Yu, J., Y. Lou, K. He, S. Yang, W. Yu, L. Han, and A. Zhao. 2016b. Goose broodiness is involved in granulosa cell autophagy and homeostatic imbalance of follicular hormones. Poult. Sci. 95:1156–1164.

Yu, J., Y. Lou, and A. Zhao. 2016c. Transcriptome analysis of follicles reveals the importance of autophagy and hormones in regulating broodiness of Zhedong white goose. Sci. Rep. 6:36877.

Zhao, Z., C. C. Lee, A. Baldini, and C. T. Caskey. 1995. A human homologue of the Drosophila polarity gene frizzled has been identified and mapped to 17q21.1. Genomics 27:370–373.

Zhou, M., Y. Du, Q. Nie, Y. Liang, C. Luo, H. Zeng, and X. Zhang. 2010. Associations between polymorphisms in the chicken VIP gene, egg production and broody traits. Br. Poult. Sci. 51:195–203.